

## Real-Time Monitoring of Mass-Transport-Related Enzymatic Reaction Kinetics in a Nanochannel-Array Reactor

Su-Juan Li, Chen Wang, Zeng-Qiang Wu, Jing-Juan Xu, Xing-Hua Xia,\* and Hong-Yuan Chen<sup>[a]</sup>

**Abstract:** To understand the fundamentals of enzymatic reactions confined in micro-/nanosystems, the construction of a small enzyme reactor coupled with an integrated real-time detection system for monitoring the kinetic information is a significant challenge. Nano-enzyme array reactors were fabricated by covalently linking enzymes to the inner channels of a porous anodic alumina (PAA) membrane. The mechanical stability of this nanodevice enables us to integrate an electrochemical detector for the real-time monitoring of the formation of the enzyme reaction product by sputtering a thin Pt film on one side of the PAA membrane. Because the enzymatic reaction is confined in a limited

nanospace, the mass transport of the substrate would influence the reaction kinetics considerably. Therefore, the oxidation of glucose by dissolved oxygen catalyzed by immobilized glucose oxidase was used as a model to investigate the mass-transport-related enzymatic reaction kinetics in confined nanospaces. The activity and stability of the enzyme immobilized in the nanochannels was enhanced. In this nano-enzyme reactor, the enzymatic reaction was controlled by mass transport if the flux was low. With an increase in

the flux (e.g.,  $> 50 \mu\text{L min}^{-1}$ ), the enzymatic reaction kinetics became the rate-determining step. This change resulted in the decrease in the conversion efficiency of the nano-enzyme reactor and the apparent Michaelis–Menten constant with an increase in substrate flux. This nanodevice integrated with an electrochemical detector could help to understand the fundamentals of enzymatic reactions confined in nanospaces and provide a platform for the design of highly efficient enzyme reactors. In addition, we believe that such nanodevices will find widespread applications in biosensing, drug screening, and biochemical synthesis.

**Keywords:** biocatalysis • glucose oxidase • kinetics • membranes • nanotechnology

### Introduction

Reactions of biomolecules spatially confined in spaces of micro-/nanometers and the corresponding bioassays have recently attracted increasing interest.<sup>[1–6]</sup> The unique properties of nanocavities and nanochannels enable them to carry out size-based chemical and biological separation,<sup>[7]</sup> label-free DNA detection,<sup>[8]</sup> enzyme-based assays,<sup>[9]</sup> and even single-molecule analysis.<sup>[10]</sup> The progress in this field would

benefit from the development of the design of new materials and novel micro-/nanoscale fabrication processes. Recently, porous inorganic membranes have attracted considerable attention for their large surface-to-volume ratio, tunable nanometer-sized pore diameters, and well-defined array conduits for the flow of low-surface-tension fluids.<sup>[11–13]</sup> In addition to the use of nanoporous membranes as templates for various designs of nanomaterials,<sup>[14,15]</sup> these membranes have evoked more interest as an application in nanofluidics, which involves molecular switch and preconcentrators.<sup>[16]</sup> As nanobioreactors, they can render biomolecules more mechanically robust, thermally stable, and more easily separable from the reaction media. Furthermore, nanochannel-array technologies based on membrane sciences can be used to independently analyze small reaction volumes, which will extend biochemical reactions to a level of fast, parallel analysis. All these advantages promise to allow the construction of high-performance and high-throughput enzyme reactors under ideal conditions.<sup>[17]</sup> Therefore, porous inorganic mem-

[a] S.-J. Li, C. Wang, Z.-Q. Wu, Prof. J.-J. Xu, Prof. X.-H. Xia, Prof. H.-Y. Chen  
Key Laboratory of Analytical Chemistry for Life Science  
School of Chemistry and Chemical Engineering  
Nanjing University, Nanjing 210093 (China)  
Fax: (+86)25-8368 6106  
E-mail: xhxia@nju.edu.cn

Supporting information for this article is available on the WWW under <http://dx.doi.org/10.1002/chem.201000318>.

branes have been extensively used to construct enzyme reactors by using various immobilization methods.<sup>[18–20]</sup>

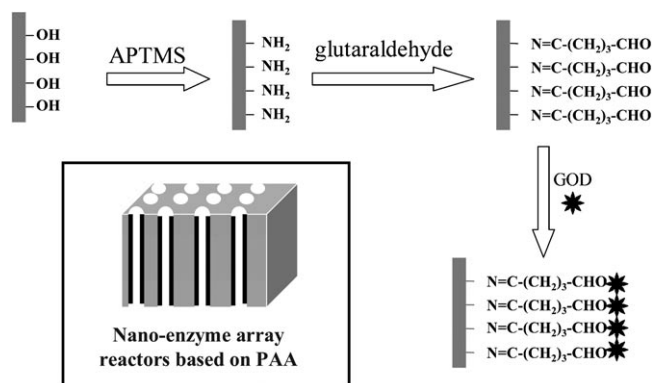
However, the implementation of an immobilized enzymatic reaction in nanometer-scaled spaces still faces challenges. Probably the biggest challenge is the limited reaction rate imposed by slow diffusion of the substrate to the enzymes within the nanocavities and nanochannels, which has been discussed previously.<sup>[12,21–22]</sup> Besides, as in the case of enzyme reactors based on a nanochannel array, once the enzymatic reaction product is formed in the nanochannels it will diffuse away to both sides of the membrane driven by the concentration gradient. As a result, only some of the reaction products could be detected on one side of the membrane, thus resulting in decreased detection sensitivity and low enzyme activity. Such phenomena would become more obvious when the product acts as an inhibitor. The most common solution to these problems is to impose a driven force to impel the solution that flows through the nanochannels by using pressure-driven or electroosmotic force.<sup>[23–24]</sup> If electrochemical methods are used to detect the enzymatic reaction product, the high driving potential for electroosmotic flow will usually couple to the electrochemical detection system and affect the electrochemical detection signals.<sup>[25]</sup> Obviously, when electrochemical detection systems are used, the pressure-driven force is preferable to accelerate mass transport in the nanochannel-array enzyme reactors. On the other hand, the development of appropriate detection systems for amenable integration into nanometer-sized membrane devices is another important challenge.<sup>[26,27]</sup>

Herein, a nano-enzyme array reactor based on a nanoporous alumina membrane was constructed and integrated with a real-time electrochemical detection system to study enzymatic reaction kinetics with a substrate that flows through the nanochannels of a porous anodic alumina (PAA) membrane. In this approach, a Pt film was sputtered on one side of the PAA membrane, which served as the working electrode to detect the formation of electrochemical species from an enzymatic reaction.<sup>[28]</sup> The double status of the PAA membrane as an enzyme reactor and detecting element is very attractive. The collection efficiency of the product at the detector could be significantly improved because the detection electrode was directly arranged close to the immobilized enzyme region in the nanopores.<sup>[29]</sup> Relative to other methods,<sup>[30]</sup> the enzyme reaction kinetics confined in the nanochannel array can be monitored in situ. Under the pressure-driven conditions, the fluid flow through the array membrane with nanometer-sized pores resulted in rapid convective mass transport of the reactants to the immobilized enzyme, thus more enzyme active sites could be accessed. The model enzyme glucose oxidase (GOD) was immobilized in the nanochannels of the PAA membrane support by covalent linking. The results demonstrated that this immobilization method could increase the stability of the immobilized enzyme, significantly decreased the amount of leaching, and allowed the immobilized enzyme to be reused. The fabrication of the electrochemical detection system will be illustrated in detail in the Experimental Sec-

tion. The kinetic parameters of the nano-enzyme reactor were determined by measuring the steady-state current response of the enzymatic reaction product at different flow rates. The present nanoreactors can be not only used as enzyme reactors, but also will find widespread applications in biosensing, drug screening, and chemical synthesis.

## Results and Discussion

**Characterization of GOD immobilized in PAA nanochannels:** When alumina, an amphoteric material, is in contact with an aqueous solution, its surface hydrolyzes to form Al–OH surface groups. These functionalized groups can be used as active sites for the immobilization of biomolecules.<sup>[27]</sup> Herein, the GOD was covalently immobilized on the inner walls of the PAA membrane by silane and glutaraldehyde coupling chemistry (Scheme 1). For the characterization of



Scheme 1. Covalent functionalization of the inner walls of the PAA membrane with GOD. APTMS = 3-aminopropyltrimethoxysilane.

the successful immobilization of GOD, FTIR was used to probe the immobilized GOD by the IR absorption of amide I and II bands. The amide I band ( $\tilde{\nu}=1700\text{--}1600\text{ cm}^{-1}$ ) is attributed to the C=O stretching vibration of the peptide linkage in the protein background. The amide II band ( $\tilde{\nu}=1625\text{--}1500\text{ cm}^{-1}$ ) results from N–H bending and C–N stretching. These absorption bands appear obviously after GOD immobilization in the PAA membrane (Figure 1). However, the IR absorption bands for the PAA membrane without GOD appear at  $\tilde{\nu}=1400\text{--}1600\text{ cm}^{-1}$ , in good agreement with other reports,<sup>[23,27]</sup> probably due to the ions with IR activity incorporated in the fabrication process. Because of the high pore density and narrow pore distance of the PAA membrane, GOD is thought to be mainly incorporated in its inner walls by the present flowing incubation method.

**Real-time detection principles for nano-enzyme reactors:** The schematic representation of the flow cell used for the flow-based nano-enzyme reactor is depicted in Figure 2A. The inlet is filled with buffer solutions and the substrate glucose is introduced into the inlet under pressure-driven force

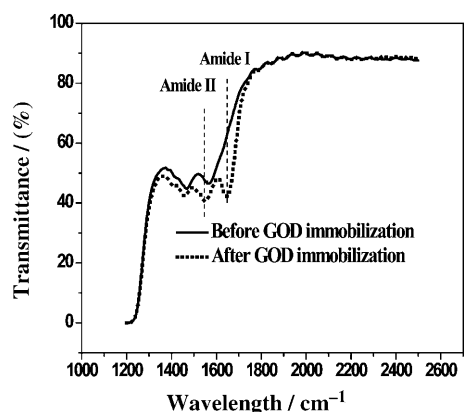


Figure 1. FTIR spectra of membranes modified with amine-functionalized silane and glutaraldehyde before and after the immobilization of GOD.

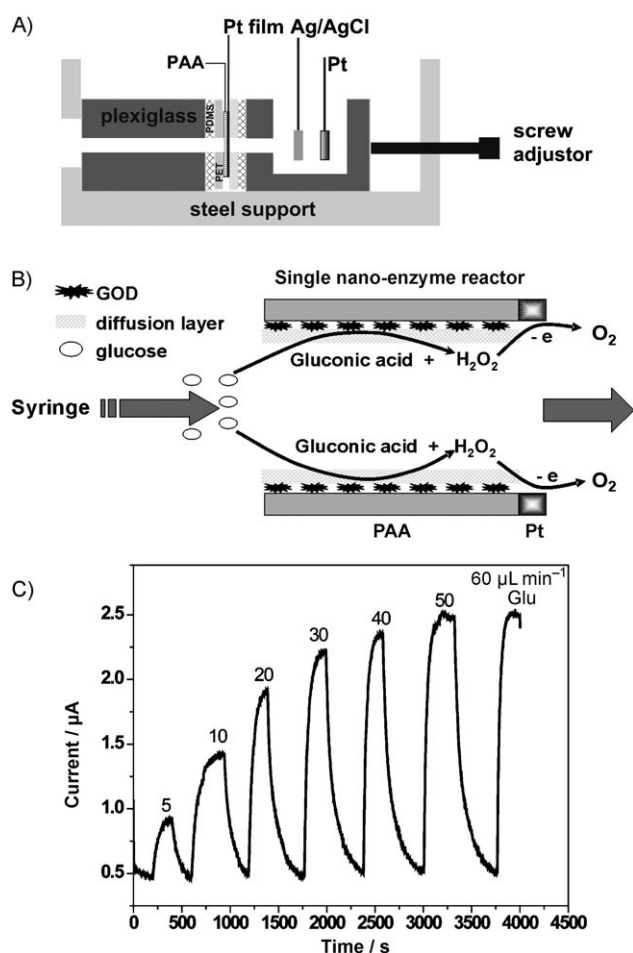


Figure 2. A) Schematic representation of the setup of the flow experiment. Pt film: the working electrode; Ag/AgCl: the reference electrode; Pt wire: the counterelectrode. The whole cell was sealed by adjusting the screw. B) A single nano-enzyme reactor demonstrates the enzymatic reaction and the principle of electrochemical detection in situ. C) Current response of 0.5 mM glucose in phosphate-buffered saline (PBS; 10 mM, pH 7.0) was detected on the Pt-film electrode at 0.70 V versus Ag/AgCl.

with a syringe pump. As glucose flows through the nano-enzyme reactor array, the enzymes immobilized in the nanochannels catalyze the oxidation of glucose with dissolved oxygen as shown by the reaction in Equation (1), thus generating the electroactive product hydrogen peroxide, which flows along the nanochannel to the end side of the PAA membrane surface coated with a Pt film under the pressure-driven conditions (as shown by the single nano-enzyme reactor in Figure 2B). In the present setup, the sputtered Pt film was deposited on the PAA membrane surface, which would not block the nanochannels of the PAA membrane (Figure 3). Therefore, when a potential of 0.70 V versus Ag/

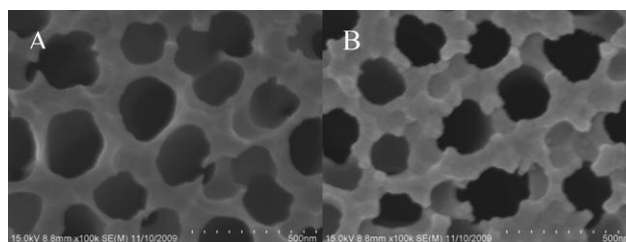
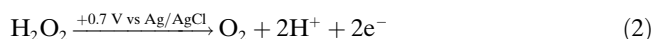
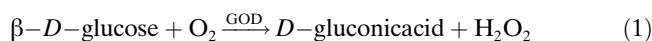


Figure 3. SEM images of the PAA membrane (pore diameter: 200 nm) before (A) and after (B) deposition of the Pt film (thickness: 100 nm).

AgCl was applied to the Pt-film working electrode, the flow-through enzymatic reaction product of  $\text{H}_2\text{O}_2$  could be real-time electrochemically detected following the electrochemical reaction shown in Equation (2). The cyclic voltamogram of  $\text{H}_2\text{O}_2$  at the Pt-film electrode is shown in Figure S1 (see the Supporting Information).



It was straightforward to monitor the current responses of a given concentration of glucose under different flux conditions (Figure 2C). It is clear that the current response increases with the flux of glucose. Once the flow of the substrate is stopped, the current response decreases to the initial value. Similarly, the current response changes with the concentration of glucose at constant flux.

To ensure that the observed increase in the current at the Pt-film electrode arises from the enzyme reaction product, the following measurements were recorded: Figure 4A shows the current responses at the Pt-film electrode when 2 mM glucose flows through the nanochannel array of the PAA membrane with and without the immobilization of GOD (the enlarged plot of current versus time is indicated in the inset). For clarity, a control experiment was also carried out (Figure 4A, curve b shows the current response of a phosphate buffer solution flowing through the GOD-immobilized PAA membrane). It is clear that there is only a negligible increase in current when 10 mM PBS flows through the GOD-immobilized PAA membrane at 200 seconds (see the enlarged inset). This current variation is probably caused by

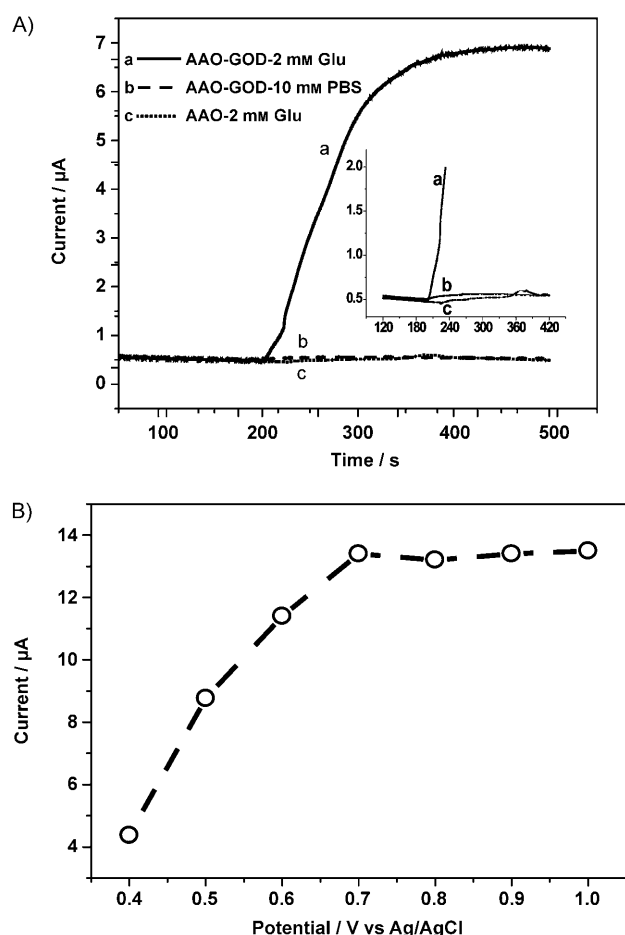


Figure 4. A) Typical current responses at the Pt-film electrode as a function of time at an applied potential of 0.7 V under different conditions with a fluid flow rate of  $20 \mu\text{L min}^{-1}$  starting at 200 s. a) Glucose (2 mM) flowing through the GOD-immobilized nanochannels array in the PAA membrane, b) PBS (10 mM, pH 7.0) flowing through the GOD-immobilized nanochannels array in PAA, c) glucose (2 mM) flowing through the PAA membrane without GOD immobilization. B) The influence of the detection potential on the response of 5 mM glucose in PBS (10 mM, pH 7.0) at the Pt-film electrode. The flow rate of the substrate was  $20 \mu\text{L min}^{-1}$ . Glu = glucose.

the turbulence that arises from the flow of the solution. Similarly, a turbulence signal appears when 2 mM glucose flows through the PAA membrane without immobilization of the enzyme (Figure 4A, curve c), thus showing that the electrooxidation of glucose that occurred at the Pt-film electrode is negligible. In contrast, when a glucose solution is introduced so that it flows through the GOD-immobilized PAA membrane starting at 200 seconds, a considerable increase in the current is observed (Figure 4A, curve a and the enlarged inset), which corresponds to the electrooxidation of hydrogen peroxide generated from the enzymatic reaction of glucose with dissolved oxygen catalyzed by the immobilized GOD in the nanochannel array of the PAA membrane. This considerable current for the electrochemical oxidation indicates that the immobilized GOD in the nanochannels of the PAA membrane retains high bioactivity. Therefore, the in-

creased current at the Pt-film electrode is mainly attributed to the electrooxidation of hydrogen peroxide generated from the enzymatic reaction in the nano-enzyme reactor. It is also noted that this current increases abruptly in the first 150 seconds after the substrate has been introduced due to the increasing concentration of glucose after its introduction. The current levels off at 220 s, thus indicating that a constant concentration of glucose in the nano-enzyme reactor has been reached. At this stage, the nano-enzyme reactor generates a steady-state concentration of the reaction product hydrogen peroxide. Fivefold parallel measurements with the introduction of 2 mM glucose into the nano-enzyme reactor shows good reproducibility (RSD = 15.5%,  $n = 5$ ). These results demonstrate that it is quite reasonable to take advantage of the steady-state current profiles to unravel the influence of the flow rate and concentration of glucose substrate on the kinetics of the enzymatic reaction confined in the nanochannel-array reactor.

Meanwhile, the detection potential for the oxidation of the enzyme reaction product hydrogen peroxide was optimized. Figure 4B shows the influence of the working electrode potential on the current response of 5 mM glucose at a constant flow of  $20 \mu\text{L min}^{-1}$ . The negligible current appears as the detection potential is lower than 0.4 V. The anodic oxidation current of hydrogen peroxide on the Pt-film electrode becomes observable at potentials more positive than 0.4 V. This current dramatically increases with the detection potential as the detection potential moves from 0.4 to 0.7 V and reaches a plateau at more positive potentials at which the electrochemical oxidation of hydrogen peroxide on this Pt-film electrode is diffusion controlled. Because an anodic detection potential that is too high will result in a higher background current, the detection potential of 0.7 V is selected to ensure a relatively high sensitivity. During these measurements, the Pt-film working electrode shows relatively good stability and reproducibility at the detection potential of 0.7 V.

**Kinetic information on the flow-rate dependence in the nano-enzyme reactor:** It is important to know the whole reaction process in the nano-enzyme reactor to understand the influence of mass transport of the substrate on the enzymatic reaction kinetic assays. As generally known from previous reports, the arrival of substrate molecules to the active site of the immobilized biocatalyst is subject to molecular diffusion within the diffusion layer  $\delta$  [Eq. (3)],<sup>[31]</sup>

$$d[S_s]/dt = m([S_b] - [S_s]) \quad (3)$$

where  $[S_s]$  is the substrate concentration at the surface of the immobilized enzyme,  $[S_b]$  is the substrate concentration in the bulk solution, and  $m$  is the mass-transfer coefficient of the substrate. A convective flow through the nanochannel array of the PAA membrane was applied to overcome the partition of the substrate between the bulk solution and the nanochannels of the membrane and the diffusional resistance of the substrate transport into the enzymes immobi-

lized in the nanochannel-array-based nano-enzyme reactor. As soon as the substrate flows over the immobilized enzyme, it reacts with the dissolved oxygen catalyzed by the immobilized enzyme. Thus, there is a decrease in the concentration of the substrate near the reaction surface, which is different from the center of the nanochannels. The concentration difference results in a reaction surface, which is called the surface diffusion layer ( $\delta$  = diffusion layer thickness; Figure 2B). It can be modulated by changing the flow rate. It is generally accepted that the thickness of the diffusion layer decreases with an increase in the fluid flow rate. Thus, an increase in the fluid flow rate results in an increase in the mass-transfer coefficient of the substrate  $m$  ( $m = D/\delta$ ;  $D$  = diffusion coefficient); accordingly, the rate at which the substrate arrives at the site in which the immobilized enzyme resides also increases, thus resulting in an increase in the reaction rate ( $d[S_s]/dt$ ).

Because the electrochemical response at the Pt-film electrode is directly proportional to the enzymatic reaction product, the flow dynamics will obviously influence both the enzymatic reaction kinetics and, in turn, the electrochemical response at the Pt-film electrode. The influence of the flux and concentration of the substrate glucose on the electrochemical response of the nano-enzyme reactor is demonstrated in Figure 5A. It is clear that at certain glucose concentrations (in the measured range 0.5–5 mM) the electrochemical response increases with the increase in fluid flux. The current increases rapidly when the fluid flux is slower than  $10 \mu\text{L min}^{-1}$  and increases slowly at the fluid flux of  $10$ – $50 \mu\text{L min}^{-1}$ . With a further increase in the fluid flux, the current response levels off. This plateau in the current increases with glucose concentration. These phenomena can be understood as follows: At the walls of the nanochannels with enzyme loaded, there is a decrease in the concentration of the analyte near the reaction surface because of the occurrence of the enzymatic reaction. More analyte can be brought to the reaction surface to compensate the consumed glucose with increasing flux, thus the current response at the Pt-film electrode increases because of the increasing amount of hydrogen peroxide product generated for a given glucose concentration. On further increasing the fluid flux, however, once the analyte flow rate exceeds the enzymatic reaction rate, no further product will be generated, thus the current response remains constant. The Levich equation<sup>[32]</sup> was used further to characterize this process. Whereas the relationship (see Figure S2B in the Supporting Information) of the current response  $I$  with flow rate ( $(\mu\text{L min}^{-1})^{1/3}$ ); based on the data in Figure 5A) demonstrates that the mass-transport process is dominant at a flow rate lower than  $10 \mu\text{L min}^{-1}$ . At a flow rate between  $10$  and  $50 \mu\text{L min}^{-1}$ , the enzymatic reaction could be controlled by both mass transport and reaction kinetics. At a flow rate higher than  $50 \mu\text{L min}^{-1}$ , the reaction is purely controlled by enzymatic reaction kinetics. If we take a fluid flux of  $50 \mu\text{L min}^{-1}$  as the alteration point of the reaction kinetics from a mass-transport-controlled to an enzymatic-reaction-controlled process, this fluid flow rate corresponds to a residence time within the membrane of

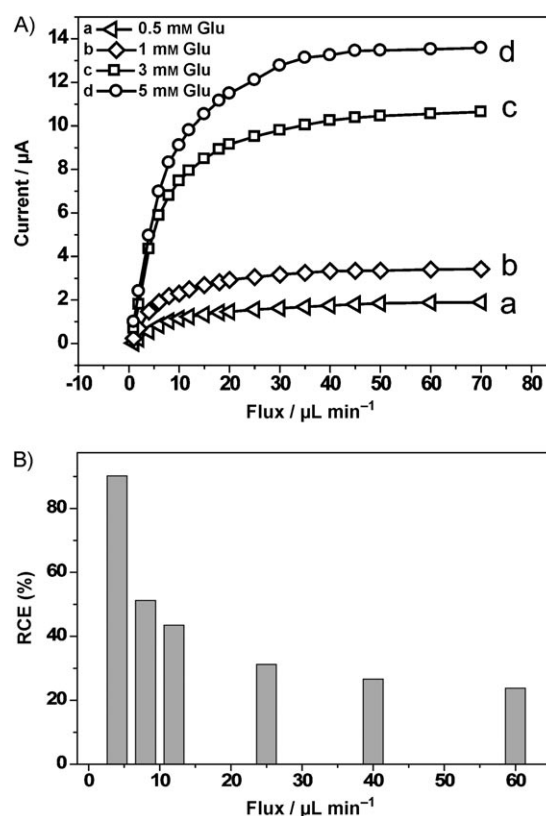


Figure 5. A) The influence of glucose flux on the electrochemical response at the Pt-film electrode at 0.70 V (the glucose concentration: a) 0.5, b) 1, c) 3, and d) 5 mM). B) RCE of 1 mM glucose with varying flow rate. The RCE was calculated from the current response of 1 mM glucose by dividing by the current response of 1 mM hydrogen peroxide at the same flow rate.

only 91 ms and a linear velocity of  $660 \mu\text{m s}^{-1}$  (exposed membrane area =  $0.0314 \text{ cm}^2$ ).

The cross-section that contains the reactive product in the nanochannels is definitive for determining the conversion efficiency of the nano-enzyme reactors. From the reactions given in Equations (1) and (2), it is clear that the electrochemical response of hydrogen peroxide is directly proportional to the reactive glucose concentration because the collection efficiency could be considered to be 100% in the nano-enzyme reactor. Because the generated hydrogen peroxide at the nanochannel surface that diffuses to the nanochannel center requires only 3.6 ms ( $1.3 \times 10^{-9} \text{ m}^2 \text{ s}^{-1}$ ),<sup>[33]</sup> its concentration distribution in the nanochannel is homogeneous. The conversion efficiency of glucose catalyzed by the immobilized enzyme in the nanochannel-array reactor can thus be evaluated by monitoring the electrochemical current of the reactive product at the Pt-film electrode under different flux conditions of the substrate. By using the conversion efficiency of 1 mM glucose as an example: if 1 mM glucose is fully converted, it is assumed that current signals for 1 mM hydrogen peroxide will be obtained. Thus, the relative conversion efficiency (RCE) of 1 mM glucose in the enzymatic reaction is defined by the ratio of the electrochemical re-

sponse of the enzymatic reaction product from 1 mM glucose to that of 1 mM hydrogen peroxide under the same conditions. The RCE results of 1 mM glucose at different flow rates are shown in Figure 5B. It is clear that the relative conversion efficiency decreases with the increase in the flux of the substrate. A higher RCE of 90% is obtained at a lower flux ( $4 \mu\text{L min}^{-1}$ ), which may be due to the reaction zone in the vicinity of the immobilized enzyme, which extends further into the central channel. Thus, most of the glucose that flows through the nanochannel-array reactor could be enzymatically converted into the product. With the increase in the substrate flux, the diffusion layer within the cross-section that contains the product decreased as discussed above; therefore, the RCE decreases with increasing flux. In addition, short residence time, the kinetically controlled process, and an increase in the flow speed play more important roles, all of which result in a lower RCE. It is expected that the RCE can be increased by decreasing the pore diameter for the whole channel to be used as a reaction zone that uses the mass-transport-controlled process. Our experimental results are consistent with the results in which the conversion efficiency was calculated for off-line detection,<sup>[11,21]</sup> thus showing the present device, that is, an integrated electrochemical detection system, is valid for real-time conversion analysis.

**Apparent enzyme activity at different flow rates:** The well-known Michaelis–Menten kinetics equation is used to describe enzyme activities in immobilized forms. For electrochemical detection, a modified version of the Michaelis–Menten equation can be expressed as<sup>[34]</sup>

$$\frac{1}{i_{\text{ss}}} = \frac{1}{i_{\text{max}}} + \frac{K_{\text{m}}}{i_{\text{max}}c} \quad (4)$$

where  $i_{\text{ss}}$  is the steady-state current of a specific concentration of the substrate,  $c$  is the substrate concentration,  $i_{\text{max}}$  is the maximum current measured under saturated substrate conditions, and  $K_{\text{m}}$  is the Michaelis constant.

At a fixed flow rate, a series of glucose concentrations of 0.05–20 mM were pumped through the GOD-immobilized nanochannel-array reactor. The steady-state current for hydrogen peroxide can be approximately used to monitor the kinetics of the enzymatic reaction in the nanochannel-array reactor. Figure 6A shows the steady-state current of the enzymatic reaction product hydrogen peroxide as a function of glucose concentration. The current increases very sharply with the concentration from 0.05 to 3 mM glucose, then increases gradually, and levels off at glucose concentrations higher than 7.0 mM. This trend shows the typical kinetic properties of enzyme reactions.

In the case of the GOD catalytic reaction, GOD catalyzes the oxidation of glucose to gluconic acid and hydrogen peroxide in a two-step mechanism. In the first step, the cofactor of the enzyme flavin adenine dinucleotide (FAD) oxidizes glucose to gluconic acid and is itself converted into the reduced form ( $\text{FADH}_2$ ). In the second step,  $\text{FADH}_2$  is oxi-

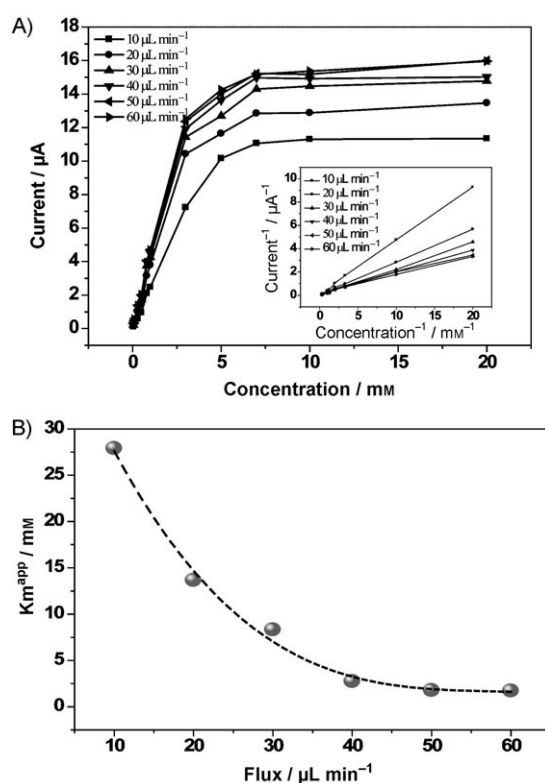


Figure 6. A) Calibration curves of the response at the Pt-film electrode at 0.7 V to glucose concentration under different flux conditions. The inset shows the Lineweaver–Burke plots for a substrate concentration range of 0.05–3 mM at different flow rates. B) The influence of flow rate on the value of  $K_{\text{m}}^{\text{app}}$ .

dized back to FAD by  $\text{O}_2$  and  $\text{O}_2$  itself is reduced to  $\text{H}_2\text{O}_2$ . According to the above reaction mechanism, the current response levels off at a high glucose concentration that may probably result from 1) the substrate is sufficient but all the active sites of the enzyme have been saturated or 2) the active sites of the enzyme are still available but the substrate  $\text{O}_2$  is deficient. We found recently that the naturally dissolved oxygen in aqueous solution is still sufficient for enzyme catalysis, even at very high enzyme concentrations (1 mM) in the nano-enzyme concentrator, and the response range for glucose extends from 0 to 15 mM.<sup>[35]</sup> These findings demonstrate that in the present nano-enzyme system with glucose in the range 0–20 mM naturally dissolved  $\text{O}_2$  is also sufficient for enzymatic catalysis. It is probable that the active sites of the immobilized enzyme with a monolayer surface concentration (ca.  $1.8 \times 10^{-13} \text{ mol cm}^{-2}$ )<sup>[36]</sup> are saturated at 7 mM glucose.

As has been mentioned, the current response increases with increasing the flow rate for a given concentration of glucose. Therefore, the detection sensitivity and detection limit of the present nanochannel-array reactor can be improved by increasing the substrate flow rate. At a flux of  $10 \mu\text{L min}^{-1}$ , the linear response of the glucose concentration ranges from 0.05 to 3 mM ( $R = 0.9967$ ) with a detection limit of 0.05 mM at a signal-to-noise ratio of 3:1 ( $S/N = 3:1$ ). This

detection limit is expected to be lower if a higher flux is used.

The apparent Michaelis–Menten constant  $K_m^{\text{app}}$ , the characteristics of enzyme reaction kinetics, can be calculated from the Lineweaver–Burk equation (Figure 6A, inset;  $R^2 > 0.99$  at any flux). The relationship between flux and  $K_m^{\text{app}}$  is demonstrated in Figure 6B. It is generally accepted that smaller values of  $K_m^{\text{app}}$  indicate better affinity of the enzyme to substrate. At a flow rate lower than  $50 \mu\text{L min}^{-1}$ , at which the whole reaction is controlled by mass transport,  $K_m^{\text{app}}$  values decrease with an increase in the substrate flux as a result of more accessibility of the enzyme (Figure 6B). With a further increase in the flow rate ( $> 50 \mu\text{L min}^{-1}$ ), the reaction-determining step changes from a mass-transport-controlled to a reaction-kinetics-controlled process, thus the appropriate  $K_m^{\text{app}}$  is nearly constant ( $1.7 \text{ mM}$ ).

For characterizing the enzyme activity in the nanoreactor, we compared the value derived from  $K_m^{\text{app}}$  for GOD immobilized in the nanochannels with the free enzyme. In bulk solutions, vigorous stirring was applied to eliminate the limitation from mass transport. Therefore, when the enzymatic reaction is the controlled process, the  $K_m$  value of GOD immobilized in a nanoenvironment ( $1.7 \text{ mM}$ ) is about sevenfold smaller than in bulk solutions (i.e.,  $11.7 \text{ mM}$ ; the results are shown in Figure S3 in the Supporting Information). This behavior might be due to the nanoconfined effects that provide an ideal environment for retaining the enzyme with high activity and stability.

**Influence of the pH level and enzyme stability:** It is known that the pH value of the solution influences enzyme conformation and bioactivity. Different pH values of buffer solution prepared with  $10 \text{ mM}$  PBS containing  $0.5 \text{ mM}$  glucose were driven through the PAA membrane to test the activity of the immobilized GOD in the nanochannels of the PAA membrane in different environments (Figure 7). The immobilized GOD exhibits the best bioactivity at pH 7.0, and the activity decreases as the solution pH deviates from this

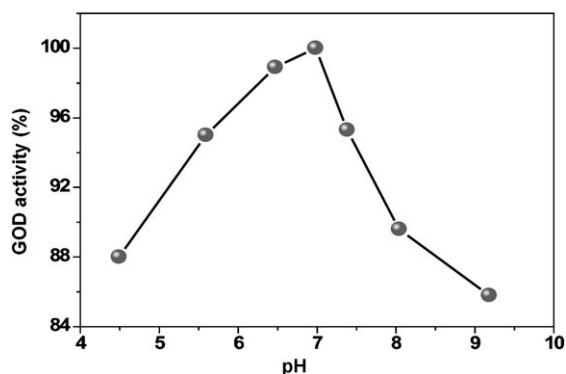


Figure 7. The influence of the solution pH value on the activity of GOD immobilized in the nanochannel-array reactor by covalent linking. The activity was calculated based on the current response of  $0.5 \text{ mM}$  glucose at the Pt-film electrode at  $0.7 \text{ V}$  and was normalized by dividing by the maximum activity (a flux of  $20 \mu\text{L min}^{-1}$  was used).

value. However, this decreasing slope in bioactivity of the immobilized GOD in the nanochannels is much slower than the results reported for the free GOD.<sup>[37–39]</sup> In the present system, the immobilized GOD still retains 85 % of the optimum activity of GOD, even at pH 9.0, thus demonstrating that the bioactivity of the immobilized GOD can be protected by the nanochannel system. The present result demonstrates that bioassays of GOD immobilized in the nanochannel array of the PAA membrane can be operated over a wide range of solution pH values without sacrificing the activity significantly.

In addition to the high activity, the reusability of the immobilized enzyme is also vital for developing high-performance reactors for biocatalysis. The enzyme immobilized within the nanochannels of the PAA membrane was stored in PBS (pH 7.0) at  $4^\circ\text{C}$ , and its stability and reproducibility were investigated by using  $5 \text{ mM}$  glucose at a flow rate of  $20 \mu\text{L min}^{-1}$  (Figure 8). After a storage time of eight days,

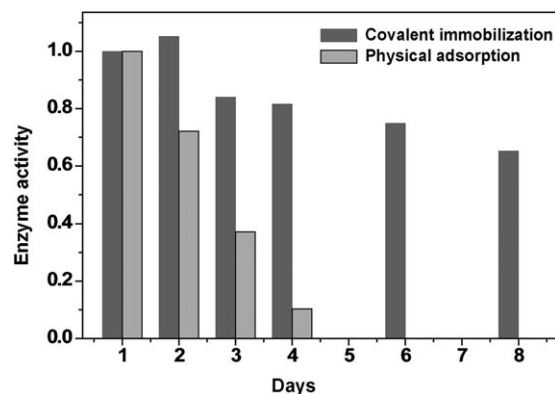


Figure 8. The stability of the nano-enzyme reactor for its performance with  $5 \text{ mM}$  glucose at a flow rate of  $20 \mu\text{L min}^{-1}$ .

the present device still retains 65 % of its initial activity. The RSD value of the electrochemical response to  $5 \text{ mM}$  glucose for four enzymatic membranes under the same conditions is  $1.6 \%$  ( $n=4$ ). These results indicate that the porous alumina membrane is biocompatible and that the nanochannels provide nanoenvironments for the immobilization of enzymes with protected biological activity. However, for the physically absorbed enzyme in the nanochannel array of the PAA membrane, the enzyme activity decreases to only 10 % of its initial value in the fourth day, probably due to the leaching of the enzyme from the membrane. In addition, the sensitivity of the current response in the case of the nanochannel-array reactor with the enzyme physically immobilized is not comparable to the covalent-coupling system due to its lower enzyme loading.

## Conclusion

In summary, we have developed a nanochannel-array enzyme reactor in which the enzymatic reaction product can

be monitored with electrochemical real-time detection. The PAA membrane provides a convenient nanofluidic platform for immobilizing active, accessible biocatalysts by using a covalent method. Therefore, the influence of mass transport on nano-enzyme reaction kinetics with a convective flow through the nanochannel array of the PAA membrane can be systematically investigated. For the model system of the oxidation of glucose by dissolved oxygen catalyzed by immobilized glucose oxidase (GOD), the current response of the electroactive product hydrogen peroxide can be detected by the Pt-film electrode arranged at the end of the nanochannels of the PAA membrane. The results show that the flow rate has a significant effect on the enzyme reaction kinetics and conversion efficiency. The enzymatic reaction is determined by mass transport at lower flux. In this case, the detection current and apparent enzyme activity is very sensitive to the flow rate. However, at a faster flux ( $>50 \mu\text{L min}^{-1}$ ), the enzymatic reaction kinetics becomes the rate-determining step and the detection current and apparent enzyme activity remain constant. These results would help us to understand the fundamentals of enzymatic reactions confined in nanospaces. The present nano-enzyme reactor integrated with a real-time detecting system could find application in various fields of bioanalysis, such as biosensors, drug screening, and chemical synthesis.

## Experimental Section

**Surface modification:** The porous anodic alumina (PAA) membrane (Whatman) with the nominal diameter of 200 nm and thickness of 60  $\mu\text{m}$  was cleaned.<sup>[40]</sup> The cleaned PAA was immersed into a mixture of 3-aminopropyltrimethoxysilane (APTMS) and acetone (10 mL; 9:1) for about 12 h, thus resulting in grafting aminopropyl functional groups onto the inner-wall surface of the PAA membrane. The excess silane solution was removed from the PAA nanochannels by rinsing with copious amounts of acetone followed by washing with deionized water. The sample was dried under a stream of nitrogen to remove any impurities and fluid. The remaining modification steps, which started from the surface-bound amines, were carried out after fabrication of the Pt-film electrode on one side of the PAA membrane and subsequently assembling the PAA membrane in the cell.

**Fabrication of the Pt-film working electrode on the PAA membrane:** The PAA-membrane-based enzyme reactor was clamped between two cells for the flow experiments (Figure 2A). It is important to make sure that the Pt-film electrode on one side of the PAA membrane is stable in the whole experimental process. Therefore, the Pt-film working electrode on the PAA membrane was fabricated as follows: Briefly, a Pt film was sputtered on one side of the PAA membrane, thereby serving as the working electrode (or detector). Sputtering to a thickness of 100 nm for the Pt film was performed with a current of 15 mA in a vacuum chamber at a pressure of  $5 \times 10^{-4}$  mbar (Ar plasma). In this case, the sputtered Pt film did not block the nanopores.<sup>[26]</sup> For easy disposal, the Pt-coated PAA membrane was sandwiched between two poly(ethyleneterephthalate) (PET) sheets (thickness: 100  $\mu\text{m}$ ; DIKA Official Limited Company, Suzhou, China) with prepunched holes (diameter: 2 mm). The holes defined the area of the membrane exposed to the contacting solutions. Cu wire (diameter: 0.2 mm) was placed in electrical contact with the Pt-coated PAA membrane by Ag conductive epoxy. Extra care had to be taken so that the Ag conductive epoxy was isolated from the solution. Finally, the membrane assembly was laminated by using a heating lamina-

tor (Zhejiang Huada Limited Company, Zhejiang, China) at 150 °C with the two prepunched holes well aligned.

**Immobilization of enzyme:** Traditional aminosilane and glutaraldehyde coupling chemistry was used for the enzyme immobilization. The APTMS-grafted PAA membrane with the fabricated Pt-film electrode was mounted in a home-made flow apparatus. A solution containing 2.5% glutaraldehyde in phosphate buffer (10 mM, pH 7.0) continuously flowed through the PAA membrane with a syringe pump (TS2-60, Multi-syringe pump, Lange, China) at a flow rate of  $20 \mu\text{L min}^{-1}$  for 1 h. Trace amounts of free glutaraldehyde possibly present in the nanochannels were removed by flowing PBS (10 mM) through the PAA membrane for 10 min to avoid cross-linking with GOD. After the above treatments, glutaraldehyde was successfully covalently coupled onto the surface amine groups on the PAA membrane, which was further used to covalently bind the amine groups of the enzymes.

The covalent immobilization of GOD was carried out by flowing a solution of GOD in pH 7 PBS ( $2.5 \text{ mg mL}^{-1}$ ; catalog no. G6125, EC 232-601-0, Type II from *Aspergillus niger*, 21 200 Units  $\text{g}^{-1}$ , purchased from Sigma-Aldrich) through the above-treated PAA membrane at a flow rate of  $2 \mu\text{L min}^{-1}$  for 1 h. Subsequently, PBS (10 mM) was pumped through the PAA membrane to remove the immobilized enzyme physically. This flow method provides a more homogeneous enzyme distribution and ensures that the enzymes are immobilized in the interior of the nanochannels of the PAA. The prepared nano-enzyme reactor could be used for enzyme assays. It could be reused with retained enzyme activity by storing in a phosphate buffer solution at pH 7.0.

**Cell assembly and pressure-driven fluid-flow measurements:** The experimental setup with the pressure-driven fluid flow is schematically illustrated in Figure 1A. Prior to the measurements, the fabricated membrane was immersed in the buffer solution for at least 30 min to ensure complete wetting. The PAA membrane was clamped between two thin poly(dimethylsiloxane) (PDMS) films and placed between two home-made half cells. The flowing channels (diameter: 2 mm) on both the half cells were aligned to the exposed holes of the PAA membrane. Importantly, the Pt-coated side of the PAA membrane was in contact with the detection cell (right-side cell), whereas the other side of the PAA membrane was in contact with the fluid inlet cell (left-side cell).

The detection half-cell contained PBS (1 mL; 10 mM, pH 7.0) and the fluid inlet half-cell was connected with a syringe pump. The Pt-film working electrode on the PAA membrane, a Pt-wire counterelectrode, and the Ag/AgCl reference electrode in the detection cell forms a three-electrode electrochemical system for electrochemical characterization. After the immobilization of the enzyme in the nanochannels of the PAA membrane as mentioned above, a constant flux of glucose solution was driven through the membrane. As a potential for the oxidation of  $\text{H}_2\text{O}_2$  was applied to the Pt-film working electrode, the enzymatic reaction product  $\text{H}_2\text{O}_2$  could be electrochemically detected by using a CHI 900 electrochemical workstation.

**Enzyme kinetics assays:** Before the enzyme reaction started, the control experiment was conducted by initially driving the buffer solution through the nanochannel-array reactor. The enzyme assays of GOD covalently immobilized in the nanochannels of the PAA membrane were conducted at various concentrations (0.05–20 mM) and flow rates of glucose. The electrochemical signals of the enzymatic reaction product  $\text{H}_2\text{O}_2$  on the Pt-film electrode at 0.7 V versus Ag/AgCl were recorded.

## Acknowledgements

This work was supported by the Grants from the National 973 Basic Research Program (2007CB714501, 2007CB936404), the National Natural Science Foundation of China (NSFC, no. 20775035, 20828006, 20890020, 20975047), and the National Science Fund for Creative Research Groups (20821063).

- [1] R. Karnik, K. Castelino, R. Fan, P. D. Yang, A. Majumdar, *Nano Lett.* **2005**, *5*, 1638–1642.
- [2] J. H. Lee, Y. A. Song, S. R. Tannenbaum, J. Y. Han, *Anal. Chem.* **2008**, *80*, 3198–3204.
- [3] Y. Q. Luo, F. Yu, R. N. Zare, *Lab Chip* **2008**, *8*, 694–700.
- [4] T. C. Logan, D. S. Clark, T. B. Stachowiak, F. Svec, J. M. J. Frechet, *Anal. Chem.* **2007**, *79*, 6592–6598.
- [5] R. B. Schoch, L. F. Cheow, J. Y. Han, *Nano Lett.* **2007**, *7*, 3895–3900.
- [6] T. Tsukahara, K. Mawatari, A. Hibara, T. Kitamori, *Anal. Bioanal. Chem.* **2008**, *391*, 2745–2752.
- [7] S. F. Yu, S. B. Lee, C. R. Martin, *Anal. Chem.* **2003**, *75*, 1239–1244.
- [8] G. Jagerszki, R. E. Gyurcsanyi, L. Hofler, E. Pretsch, *Nano Lett.* **2007**, *7*, 1609–1612.
- [9] V. Vamvakaki, N. A. Chaniotakis, *Biosens. Bioelectron.* **2007**, *22*, 2650–2655.
- [10] N. Mitchell, S. Howorka, *Angew. Chem.* **2008**, *120*, 5647–5650; *Angew. Chem. Int. Ed.* **2008**, *47*, 5565–5568.
- [11] W. S. Fu, A. Yamaguchi, H. Kaneda, N. Teramae, *Chem. Commun.* **2008**, 853–855.
- [12] D. M. Dotzauer, J. H. Dai, L. Sun, M. L. Bruening, *Nano Lett.* **2006**, *6*, 2268–2272.
- [13] E. Dujardin, T. W. Ebbeson, H. Hiura, K. Tanigaki, *Science* **1994**, *265*, 1850–1852.
- [14] W. Chen, X. H. Xia, *Adv. Funct. Mater.* **2007**, *17*, 2943–2948.
- [15] Z. H. Wen, Q. Wang, J. H. Li, *Adv. Funct. Mater.* **2008**, *18*, 959–964.
- [16] R. Mukhopadhyay, *Anal. Chem.* **2006**, *78*, 7379–7382.
- [17] S. Hudson, J. Cooney, E. Magner, *Angew. Chem.* **2008**, *120*, 8710–8723; *Angew. Chem. Int. Ed.* **2008**, *47*, 8582–8594.
- [18] M. Darder, P. Aranda, M. Hernandez-Velez, E. Manova, E. Ruiz-Hitzky, *Thin Solid Films* **2006**, *495*, 321–326.
- [19] Z. P. Yang, S. H. Si, H. J. Dai, C. J. Zhang, *Biosens. Bioelectron.* **2007**, *22*, 3283–3287.
- [20] G. B. Oliveira, J. L. Lima Filho, M. E. Cavalcante Chaves, W. Mendes Azevedo, L. Bezerra Carvalho, Jr., *React. Funct. Polym.* **2008**, *68*, 27–32.
- [21] S. Datta, C. Cecil, D. Bhattacharyya, *Ind. Eng. Chem. Res.* **2008**, *47*, 4586–4597.
- [22] V. Smuleac, D. A. Butterfield, D. Bhattacharyya, *Langmuir* **2006**, *22*, 10118–10124.
- [23] J. H. Dai, G. L. Baker, M. L. Bruening, *Anal. Chem.* **2006**, *78*, 135–140.
- [24] W. Chen, J. H. Yuan, X. H. Xia, *Anal. Chem.* **2005**, *77*, 8102–8108.
- [25] K. Wang, W. Z. Jia, X. H. Xia, *ChemPhysChem* **2008**, *9*, 2109–2115.
- [26] M. S. Kang, C. R. Martin, *Langmuir* **2001**, *17*, 2753–2759.
- [27] X. Wang, S. Smirnov, *ACS Nano* **2009**, *3*, 1004–1010.
- [28] S. Kuwabata, C. R. Martin, *Anal. Chem.* **1994**, *66*, 2757–2762.
- [29] J. J. Gooding, *Electrochem. Commun.* **1999**, *1*, 119–123.
- [30] M. Delvaux, S. Demoustier-Champagne, A. Walcarius, *Electroanalysis* **2004**, *16*, 190–198.
- [31] P. Richter, B. L. Ruiz, M. Sanchez-Cabezudo, H. A. Mottola, *Anal. Chem.* **1996**, *68*, 1701–1705.
- [32] J. J. Gooding, E. A. H. Hall, *Anal. Chem.* **1998**, *70*, 3131–3136.
- [33] T. Henzler, E. Steudle, *J. Exp. Bot.* **2000**, *51*, 2053–2066.
- [34] C. Y. Deng, M. R. Li, Q. J. Xie, M. L. Liu, Y. M. Tan, X. H. Xu, S. Z. Yao, *Anal. Chim. Acta* **2006**, *557*, 85–94.
- [35] C. Wang, S. J. Li, Z. Q. Wu, J. J. Xu, H. Y. Chen, X. H. Xia, *Lab Chip* **2010**, *10*, 639–646.
- [36] D. T. Pierce, P. R. Unwin, A. J. Bard, *Anal. Chem.* **1992**, *64*, 1795–1804.
- [37] S. Rauf, A. Ihsan, K. Akhtar, M. A. Ghauri, M. Rahman, M. A. Anwar, A. M. Khalid, *J. Biotechnol.* **2006**, *121*, 351–360.
- [38] Z. F. Li, E. T. Kang, K. G. Neoh, K. L. Tan, *Biomaterials* **1998**, *19*, 45–53.
- [39] L. Ying, E. T. Kang, K. G. Neoh, *J. Membr. Sci.* **2002**, *208*, 361–374.
- [40] M. Nagale, B. Y. Kim, M. L. Bruening, *J. Am. Chem. Soc.* **2000**, *122*, 11670–11678.

Received: February 5, 2010  
Published online: July 19, 2010